OIKOS

Research article

Cross-scale scaling-law analyses for the heterogeneity and diversity of animal gut microbiomes from community to landscape

Zhanshan (Sam) Ma[1,2,4] **and Aaron M. Ellison**[1,3]

[1]Harvard University, Harvard Forest, Petersham, MA, USA
[2]Computational Biology and Medical Ecology Lab, Center for Excellence in Animal Evolution and Genetics, Kunming Institute of Zoology, Chinese Academy of Sciences, Kunming, China
[3]Sound Solutions for Sustainable Science, Boston, MA, USA
[4]Department of Entomology, College of Plant Protection, Hebei Agricultural University, Baoding, China

Correspondence: Zhanshan (Sam) Ma (ma@vandals.uidaho.edu)

Oikos
2025: e10598
doi: 10.1111/oik.10598
Subject Editor: Pedro Peres-Neto
Editor-in-Chief: Pedro Peres-Neto
Accepted 03 October 2024

Diversity and heterogeneity often are conflated but are fundamentally different. An aphorism proposed by Shavit and Ellison (2021; J. Phil. 118: 525–548) for distinguishing them is that 'a zoo is diverse whereas an ecosystem is heterogeneous.' That is, a zookeeper measuring diversity simply enumerates the different types of animals; interactions are not expected to occur between animals separated by fences or other barriers. In contrast, measures of heterogeneity ought to include both interspecific interactions and relationships between species and their heterogeneous habitats. Here, we use cross-scale, dual scaling-law analyses of heterogeneity and diversity of animal gut microbiomes (AGMs) to address three objectives: 1) estimate the spatial heterogeneity and diversity of animal-gut microbiomes; 2) analyze influences of phylogeny and diets on scaling of diversity and heterogeneity; 3) explore mechanistic differences between diversity and heterogeneity in AGMs. From 4903 AGM samples collected from 318 animal species covering all six classes of vertebrates and four major classes of invertebrates, we estimated that ≈640 000 operational taxonomic units (OTUs or 'species') make up the pool of microbial species that could inhabit animal guts, among which ≈8000 are relatively common and ≈800 are dominant. The gut of any single animal, however, includes only 0.01–0.5% of the total species pool. We applied Ma's diversity-area relationship for scaling diversity, and extend Taylor's power law and Luna et al.'s (2020; Diversity 12: 86) interaction diversity for scaling heterogeneity. At the community scale, phylogeny significantly influenced heterogeneity, but diets did not. Phylogeny and diets had limited influence on diversity at both community and landscape scales. We demonstrated that diversity and heterogeneity measure two different properties. Further, differences in scaling of diversity and heterogeneity are a result of heterogeneity being primarily the result of evolved dispersal behavior and interspecific interactions, whereas diversity results from abundances controlled on ecological time scales.

NORDIC SOCIETY OIKOS

www.oikosjournal.org

Keywords: Animal gut microbiome, diet, diversity, diversity-area relationship, heterogeneity, hill numbers, interactions, phylogeny, Taylor's power law

Introduction

'Diversity' (either species richness [S] or an abundance-weighted measures such as Shannon–Weiner's H', evenness [$H'/\ln(S)$], or their Hill-number equivalents) is a fundamental ecological property of communities, landscapes and ecosystems (Magurran and McGill 2011, Chao et al. 2014a, b). 'Heterogeneity' also is a fundamental property of landscapes and ecosystems, where it usually refers to spatial heterogeneity (e.g. patchiness, spatial turnover in diversity; Kolasa and Pickett 1991, Li and Reynolds 1995, Cohen and Saitoh 2016). Insofar as diversity (usually S) and heterogeneity are considered together, environmental heterogeneity is thought to be a cause (or predicate; see Shavit and Ellison 2021) of diversity in communities, landscapes and ecosystems. In practice, two other measures of diversity – unevenness (1–evenness) and beta diversity (the difference between, or quotient of, global and local diversity; Ellison 2010) – often are synonymized with heterogeneity. However, a clearer distinction between diversity and heterogeneity has provided new insights into the structure and dynamics of communities and ecosystems (Shavit and Ellison 2021). Shavit and Ellison (2021) also suggested an aphorism for distinguishing between diversity and heterogeneity: 'a zoo is diverse whereas an ecosystem is heterogeneous.' That is, a zookeeper measuring diversity simply enumerates the different types of animals; interactions between animals separated by fences or other barriers are irrelevant to measures of diversity. Shavit and Ellison (2021) argued that in contrast to a zookeeper's diversity, measures of heterogeneity ought to include both interspecific interactions and relationships between species and their heterogeneous habitats (Luna et al. 2020).

In this study, we recognize commonalities and differences between diversity and heterogeneity, and identify them using a unified mathematical model (Ma and Taylor 2020) extended from Taylor's power law (TPL; Taylor 2019), the species–area relationship (SAR; Connor and McCoy 1979), and the diversity–area relationship (DAR; Ma and Ellison 2021) applied to a very large dataset of the animal-gut microbiome (AGM; see Box 1 for a full list of abbreviations and acronyms used). We estimate the global richness of operational taxonomic units (OTUs, or 'species') in the AGM, the number of total species, common (or abundant; sensu Chao and Colwell 2022) species, and highly abundant or dominant species (sensu Ma and Ellison 2018, Chao and Colwell 2022) at the community and regional (landscape) scales. We also use the extension from the SAR to the DAR (Ma 2018a) to estimate potential (or 'dark') diversity: the contribution to the global scale estimate of biodiversity of species that are present in the (habitat-specific) regional species pool but locally absent or undetected (Partel et al. 2011, Real et al. 2017).

For heterogeneity, we start with extensions of TPL (of Ma 2012, 2015, Oh et al. 2016, Li and Ma 2019, Ma and Taylor 2020) that have been used to quantify spatial heterogeneity and temporal stability. We then extend this approach to characterize landscape-scale heterogeneity. These metrics for heterogeneity require information on distance and dispersal or movement that are associated with spatiotemporal distribution of abundances (Taylor and Taylor 1977, Taylor 1981a, b). We also use Luna et al.'s (2020) measure of 'interaction diversity' as a measure of heterogeneity, although it does not account for differences in species abundances (cf. Shavit and Ellison 2021). We revise Luna et al.'s (2020) interaction diversity to use Hill numbers (Chao et al. 2014a, b), apply it to core-periphery networks (CPNs; Ma and Ellison 2019) of the AGM, and compare it with the results of our extension and application of TPL to measure heterogeneity.

Finally, our common mathematical framework allows to compare our results across spatial scales, to investigate how evolutionary history (i.e. phylogeny) and diets influence scaling of diversity and heterogeneity, and to investigate similarities, differences and relationships between the scaling of parameters of diversity and heterogeneity.

Box 1. Acronyms and abbreviations used in this paper

AGM Animal-gut microbiome
CPN Core–periphery network
DAR Diversity–area relationship
DTAR Diversity–time–area relationship
H' Shannon–Weiner diversity $= -\sum p_i \ln p_i$
${}^qH_2$ Interaction diversity of Hill-number order q
${}^qD_{max}$ Estimated asymptotic diversity (potential) of Hill-number order q
${}^qLGD$ Ratio of local to global diversity of Hill-number order q
OTU Operational taxonomic unit; a.k.a. microbial species
S Species richness
SAR Species–area relationship
STAR Species–time–area relationship
TPL Taylor's power law

Material and methods

Datasets

We used datasets from 91 published studies that included 6900 samples of 16s-rRNA sequencing reads from AGMs spanning 5 phyla and 19 classes (Ma and Ellison 2024). Of these samples, we excluded any that were not collected from the gastrointestinal tract or from animals that had been treated with antibiotics. After this

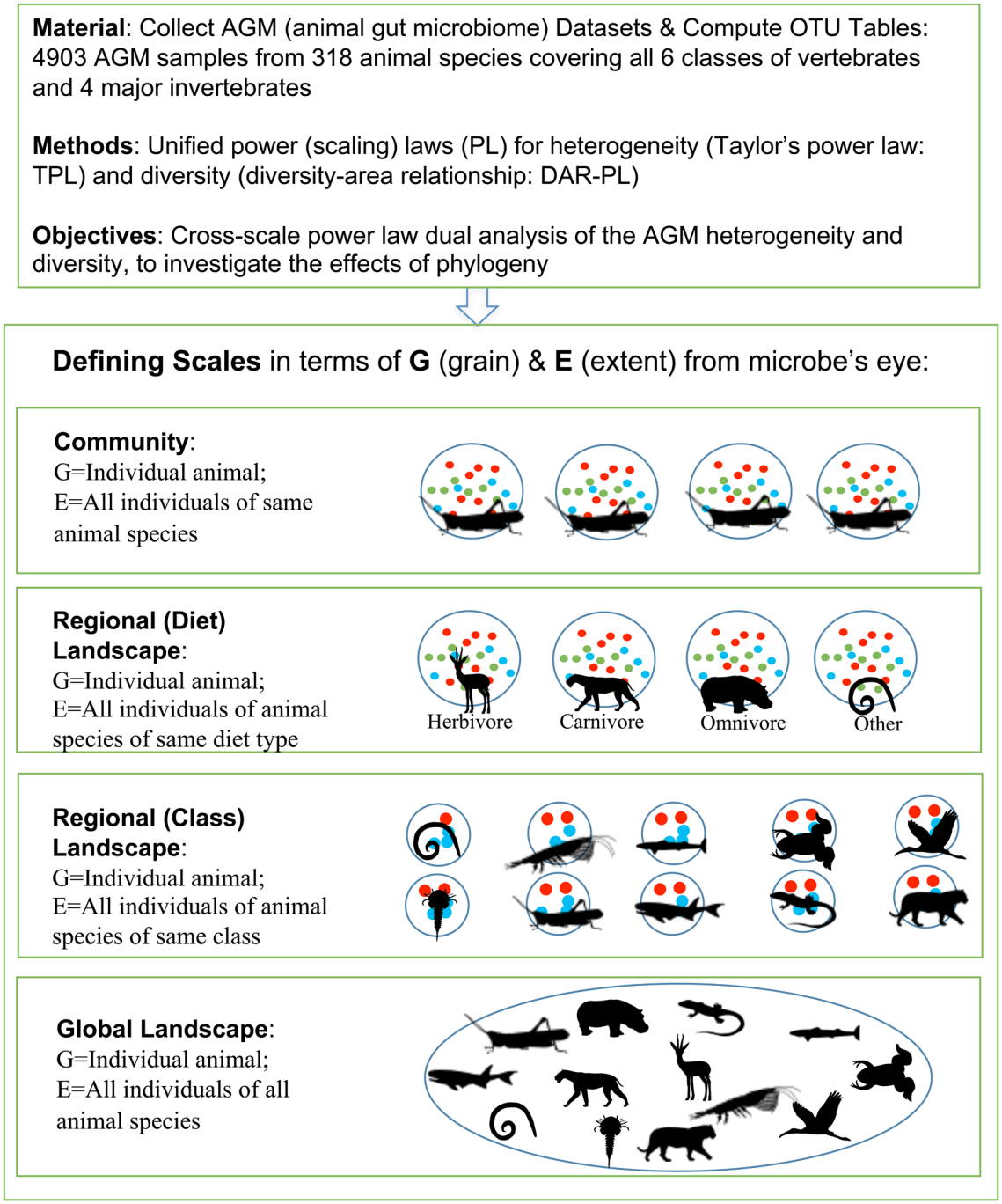

Figure 1. Grain and extents of the three microbial spatial scales at which we measured diversity and heterogeneity.

pre-screening, we were left with 4903 samples, of which 1421 were from carnivores, 1229 from herbivores, 1473 from omnivores, and 320 from animals with 'other' diet types (e.g. parasites). We then used QIIME-2 (ver. 2018.6.0: Bolyen et al. 2019) to recompute the OTU tables at the 97% similarity level. Phylogenies were visualized with the 'ape' (Paradis et al. 2004) and 'ggtree' (Yu et al. 2017) R packages. We obtained estimates of phylogenetic timeline ('taxon age') from https://timetree.org (Kumar et al. 2017).

Microbial scales

Spatial scale is one of ecology's central organizing principles (Levin 1992). Because diversity and heterogeneity depend on scale, we need to specify the scale(s) of our analysis. Grain (the finest resolution of the data) and extent (the area covered by a study) are the primary scaling factors that we need to identify (Li and Reynolds 1995), and both vary with observers (Turner and Gardner 2015). That is, the landscape of a microbe is very different from the landscape of a human.

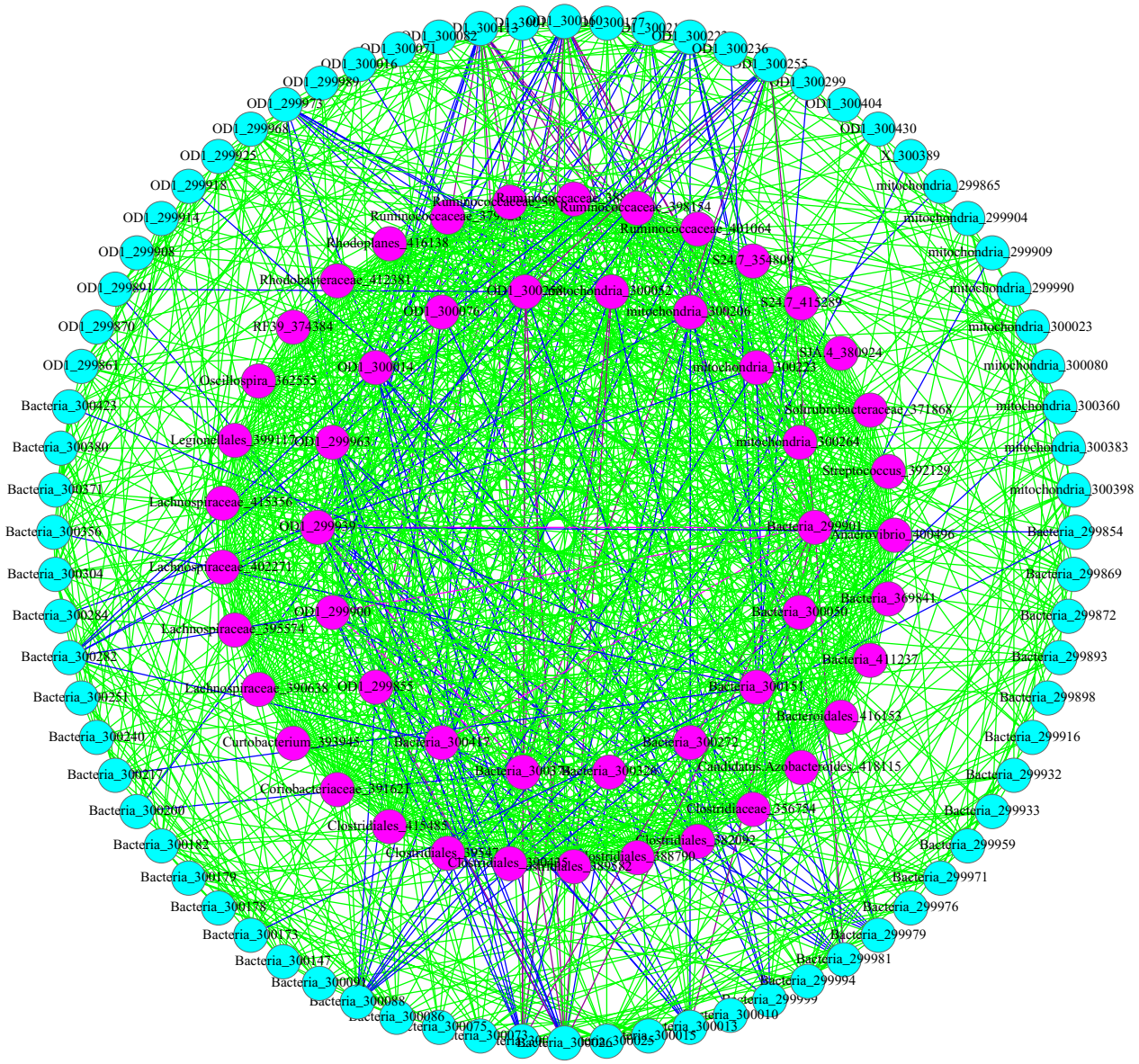

Figure 2. An example of a core–periphery network (CPN) of an animal-gut microbiome (AGM) constructed to enable the calculation of heterogeneity using Eq. 11. This CPN is of the samples from the insect order *Orthoptera*, and illustrates two kinds of nodes: (i) core nodes (magenta circles, inside); and (ii) periphery nodes (cyan circles, outside). Six kinds of interactions (links) between nodes are illustrated: (i) positive core–core links (green lines); (ii) positive periphery–periphery links (green lines); (iii) negative core–core links (red lines); (iv) negative periphery–periphery links (red lines); (v) positive core–periphery links (blue lines); and (vi) negative core–periphery links (magenta lines).

We explored patterns of diversity and heterogeneity at three spatial scales: the community, regional landscape and global scales (Fig. 1). The spatial grain for all three of these scales was defined as an individual animal host. At the community scale, we defined the extent as all the individuals of a single animal species in our sample. At the global scale, we defined the extent as all the individual animals in all species in our sample. In between we defined two regional (landscape) scales – one based on diet (the extent defined by all animal species sharing a single diet type) and the other based on taxonomic class (the extent defined by all the animal species in a single class).

Scale-dependent analyses of spatial heterogeneity

We analyzed the spatial heterogeneity using an extension of Taylor's power law,

$$V = am^b \tag{1}$$

where m is the mean abundance of a group of populations, V is its variance, b is a species-specific parameter that measures population aggregation, and a is a parameter influenced by sampling methods (Taylor 1961, 1984).

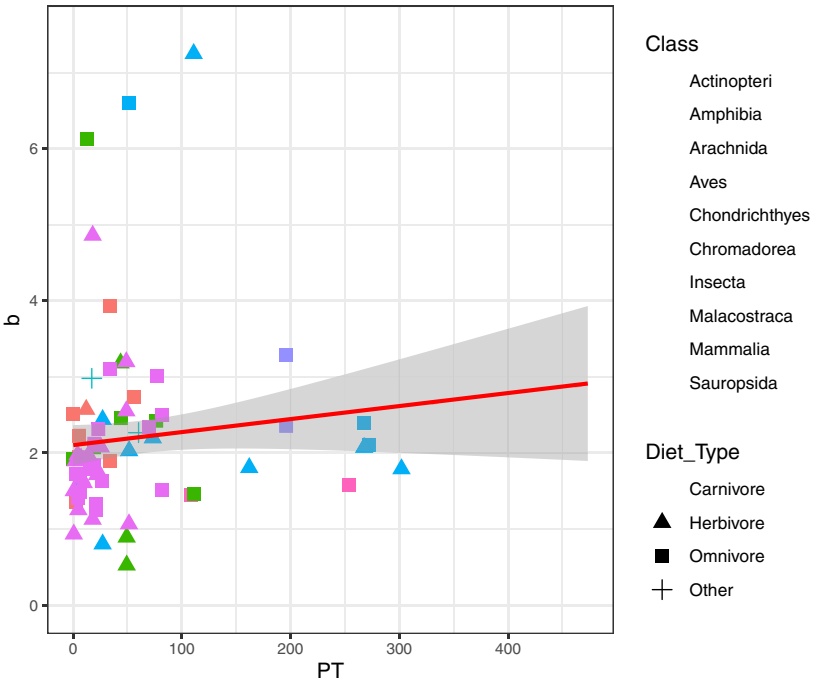

Figure 3. Relationship between estimated taxon age (phylogenetic timeline, PT) and the scaling parameter b from Eq. 2 fit to the AGM of each animal species in ten classes (indicated in different colors) and four diet types (indicated with different symbol shapes). The full phylogenetic tree of these taxa is shown in the Supporting information.

Heterogeneity at the community scale

Ma (2015) extended the interpretation of Eq. 1 to the microbial community scale as:

$$V_i = am_i^b, \quad i = \{1,2,\ldots,N\} \tag{2}$$

where m_i is the mean of population abundances of all microbial species in the i-th community carried by the i-th animal individual (i.e. the mean population size [abundance] per microbial species in the community); V_i is the corresponding variance; N is the number of total communities sampled (i.e. the number of animal individuals sampled and assuming each individual is sampled once). We fit Eq. 2 to the AGMs of each of 145 animal species. Because the data did not satisfy the assumptions of normality and homoscedasticity, we used a two-factor non-parametric ANOVA (i.e. the Scheirer–Ray–Hare test as implemented in the `rcompanion` package; Mangiafico 2024) to test for the influences of diet type and taxon age on the scaling parameter, b.

Table 1. Average community-level heterogeneities of the AGM of each combination of taxonomic class and diet group of animals (see Fig. 1 for illustration of scales). Heterogeneity is measured as the mean over all individuals of each species within each taxonomic class or diet group of parameters b and ln(a) from the linearized Eq. 2 (parameter estimates, model fits, sample sizes, and estimated taxon age for each of the AGMs of 145 species are listed in the Supporting information). An — in a cell indicates either no animals in that class or group or too few animals for reliable estimation. *N is the total number of animal species in each row (all animals in a class) or column (all animals within a diet group).

	Diet group (*N)									
	Carnivore (34)		Herbivore (44)		Omnivore (57)		Other (10)		Class mean	
Class (*N)	b	ln(a)	b	ln(a)	b	ln(a)	ln(a)	ln(a)	b	ln(a)
Chromadorea (3)	—	—	—	—	—	—	8.666	8.666	2.348	8.666
Arachnida (5)	2.625	4.409	—	—	—	—	5.196	5.982	2.341	5.196
Malacostraca (2)	—	—	—	—	2.823	4.315	4.315	—	2.823	4.315
Insecta (31)	2.273	11.267	2.725	3.856	2.498	3.264	5.578	3.926	2.425	5.578
Chondrichthyes (4)	2.052	9.643	—	—	—	—	9.643	—	2.052	9.643
Actinopterygii (24)	2.319	3.831	2.991	4.517	2.290	3.810	4.052	—	2.533	4.052
Amphibia (1)	1.707	4.944	—	—	—	—	4.944	—	1.707	4.944
Sauropsida (5)	1.516	7.632	1.322	7.181	1.514	5.979	6.930	—	1.450	6.930
Aves (14)	NA	NA	1.637	6.901	3.864	1.311	4.681	5.831	2.711	4.681
Mammalia (56)	2.048	5.576	1.877	5.039	1.906	6.392	5.669	—	1.944	5.669
Diet group mean	2.077	6.757	2.110	5.499	2.482	4.178	5.968	6.101	2.233	5.968

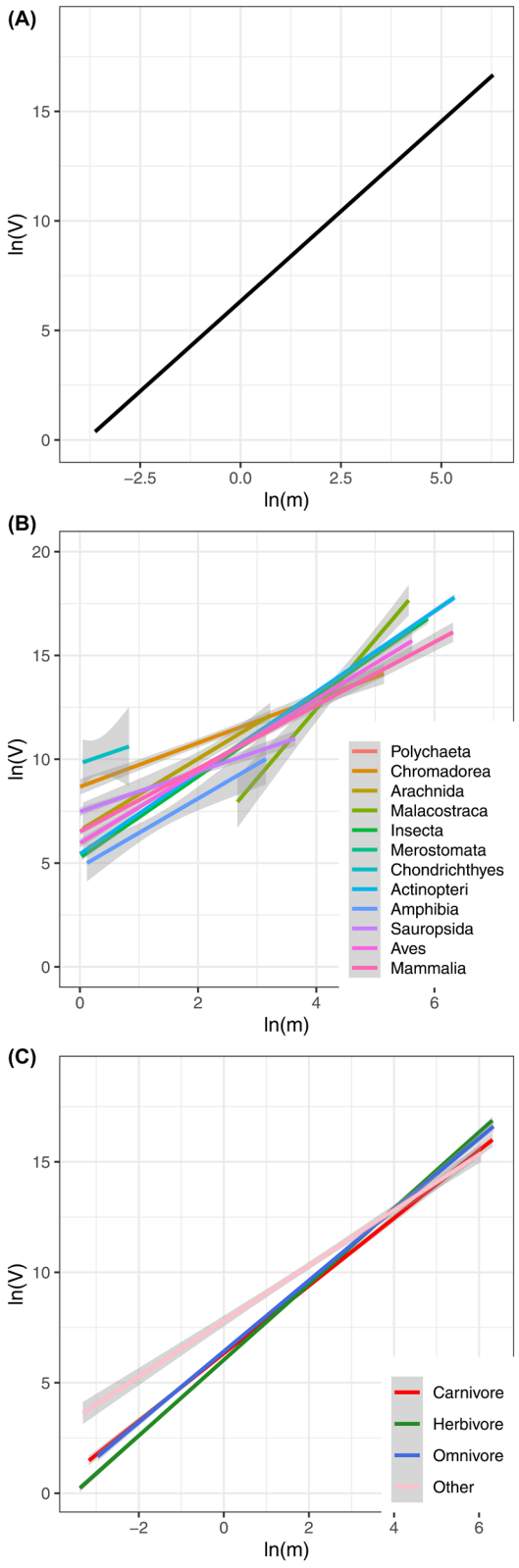

Figure 4. Heterogeneity (slope of the relationship between abundance [$\ln(m_{ij})$] and variance [V_{ij}]) fitted using Eq. 3 for (A) all microbial species in the studied AGMs, (B) AGMs in each taxonomic class, and (C) AGMs in each diet group.

Heterogeneity at the landscape and global scales

For regional and global scales, we extended Eq. 1 to:

$$V_{ij} = am_{ij}^{b} \quad i = \{1,2,\ldots,N_j; j = 1,2,\ldots,S\} \tag{3}$$

where m_{ij} is the mean of population abundances of all microbial species in the i-th individual animal (i.e. the community) of animal species j; V_{ij} is the corresponding variance; N_j is the number of total communities sampled from species j; and S is the number of animal species. Unlike in the community-scale analysis (Eq. 2), however, S in Eq. 3 includes multiple host species: all species within a single class or diet type (regional scale; Fig. 1) or all species in the entire dataset (global scale; Fig. 1). We fit Eq. 3 to the AGMs of 11 animal classes, the four defined diet types, and the entire dataset.

Scale-dependent analysis of diversity

Estimating diversity using Hill numbers

We used Hill numbers to compute estimates of species diversity (Chao et al. 2014a, b). Hill numbers are defined as:

$${}^{q}D = \left(\sum_{i=1}^{S} p_i^{q} \right)^{1/(1-q)} \tag{4}$$

where D is the diversity in Hill numbers, q is the order number of diversity, S is the number of species (or OTUs), and p_i is the relative abundance of species (OTU) i. q determines the sensitivity of the Hill numbers to the relative frequencies of species abundances. When $q = 0$, ${}^{0}D = S$ (i.e. species richness). When $q = 1$, ${}^{1}D = e^{H'}$, the exponential of Shannon–Wiener's H', and when q = 2, ${}^{2}D = \frac{1}{\cdot p_i^{2}}$, which is the reciprocal of Simpson's diversity index. ${}^{0}D$ is equivalent to species richness (S), ${}^{1}D$ gives an estimator of abundant or common species, and ${}^{2}D$ gives an estimator of highly abundant or dominant species (Chao and Colwell 2022).

Diversity–area relationships (DARs)

We used the Hill-number estimates of species diversity to examine diversity–area relationships (DARs; Ma 2018a, Ma and Ellison 2021) in the entire dataset and separately for communities and regions (taxonomic classes and diet groups). Here, we consider 'area' (A) to be equivalent to the number of samples in a given spatial extent of AGMs. We used two different models to fit the DAR: a power-law model (Eq. 5) and a power-law with exponential cut-off model (Eq. 6):

$${}^{q}D = cA^{z} \tag{5}$$

$${}^{q}D = cA^{z} \exp(dA), \tag{6}$$

Table 2. Regional-scale heterogeneities of the AGM in each taxonomic class of animals (see Fig. 1 for illustration of scales). Heterogeneity was measured as the parameters b and ln(a) from fitting the linearized Eq. 3 to the n AGMs in N animal species in each class. The amount of variance explained by each model (R^2) and its associated p-value are given in the last two columns of the table.

Class	b	ln(a)	N	n	R^2	p-value
Chromadorea	1.200	8.257	84	215	0.618	<0.001
Arachnida	1.089	8.096	10	45	0.489	<0.001
Malacostraca	1.451	8.034	1	30	0.897	<0.001
Insecta	1.554	6.678	86	646	0.702	<0.001
Chondrichthyes	2.009	9.394	5	32	0.861	<0.001
Actinopterygii	1.890	5.607	52	1271	0.929	<0.001
Amphibia	1.653	4.804	3	21	0.607	<0.001
Sauropsida	1.406	7.114	12	284	0.514	<0.001
Aves	1.623	6.152	35	531	0.584	<0.001
Mammalia	1.697	6.414	135	1443	0.794	<0.001
Mean	1.592	7.277				
SE	0.089	0.456				

where ${}^qD$ is the Hill number of order q; A is the number of samples in a given spatial extent of AGMs; and c and z are estimated parameters. In Eq. 7, d is another fitted parameter; the exponential decay term exp (dA) leads to an asymptotic estimator of maximum diversity when A is very large (Ma 2018a, Ma and Ellison 2021).

After fitting Eq. 6 to the data at the different scales, we used the estimated parameters to determine the asymptotic (maximum) diversity of order q (${}^qD_{max}$; Eq. 7) and, from ${}^qD_{max}$, the ratio of local to global diversity of order q (^{q}LGD: Eq. 8):

$$ {}^qD_{\max} = c\left(-\frac{z}{d}\right)^z \exp(-z) = cA_{\max}^z \exp(-z) \tag{7}$$

$$ {}^qLGD = {}^q c / {}^q D_{\max}, \tag{8}$$

where $A_{\max} = -\frac{z}{d}$ is the number of individuals (samples) needed to reach the maximum diversity, and c, d and z are the parameters estimated from Eq. 6.

We used the non-parametric Scheirer–Ray–Hare test to test for the influences of diet type and taxonomic class on the DAR scaling parameters at the community scale.

Table 3. Regional-scale heterogeneities of the AGM in each diet group of animals (see Fig. 1 for illustration of scales). Heterogeneity was measured as the parameters b and ln(a) from fitting the linearized Eq. 3 to the n AGMs in N animal species in each diet group. The amount of variance explained by each model (R^2) and its associated p-value are given in the last two columns of the table.

Diet group	b	ln(a)	N	n	R^2	p-value
Carnivore	1.555	6.368	81	1421	0.687	0.000
Herbivore	1.759	6.132	106	1258	0.876	0.000
Omnivore	1.633	6.433	137	1539	0.766	0.000
Other	1.257	7.792	121	331	0.704	0.000
Mean	1.551	6.681				
SE	0.107	0.376				

The importance of taxon age for the DAR

Ma (2018b) extended the classic species–time–area relationship model (STAR; Rosenzweig 1995) to a more general diversity–time–area relationship (DTAR):

$$ {}^qD = cA^zT^w \tag{9}$$

where ${}^qD$ is the diversity measured with Hill numbers of order q, A is the area, T is the time, z and w are scaling exponents corresponding to area and time, respectively, and c is a parameter that is equal to the diversity when T = 1 and A = 1, i.e. a diversity at an initial point in time and space. Equation 9 lets us include taxon age to look at the evolution of the AGM DAR through time; we set the accumulation order of the species to be equivalent to the ordered taxon age. The DTAR model can include effects of space and time, so we consider it to be a unified model for exploring effects of scaling on diversity.

Equation 9 was fit to the Hill-number diversity of the AGMs from 195 animal species, including 65 carnivores, 65 herbivore and 65 omnivores. These species were selected from the total of 224 animal species in our dataset for which had reliable estimates of taxon age (Ma and Ellison 2024); 29 species were excluded to balance the sample sizes among carnivores, herbivores, and omnivores. To eliminate random noise from arbitrarily ordering the diet types, and because the estimation of the parameters in Eq. 9 (as with Eq. 7) may be influenced by the choice of starting accumulation point, we repeated the model-fitting 100 times by using randomly permutated areas (here, microbial samples), and then computed the average value of the parameters from the permutations.

Linking diversity and heterogeneity with interactions

Luna et al. (2020) proposed a metric for measuring interaction diversity, which Shavit and Ellison (2021) considered as one measure of heterogeneity for a community:

$$ H_2 = -\sum_i \sum_j \left(\frac{a_{ij}}{m} \ln \frac{a_{ij}}{m}\right), \tag{10}$$

Table 4. Scaling parameter z and Hill number estimates of maximum species diversity for $q=0$ (species richness), and three abundance-weighted measures ($q \in \{1, 2, 3\}$) for the AGM in all the samples pooled (global scale), samples from the different taxonomic classes, and samples from the different diet groups (regional scales). Additional parameter estimates and model fits are given in the Supporting information.

	$q=0$		$q=1$		$q=2$		$q=3$	
	z	D_{max}	z	D_{max}	z	D_{max}	z	D_{max}
All samples	0.91	603 937	0.72	8114	0.63	799	0.58	325
Classes								
Chromadorea	0.91	11 347	0.59	144	0.51	46	0.47	31
Arachnida	1.01	6988	0.71	120	0.61	48	0.57	36
Malacostraca	1.02	7411	0.43	—	0.21	—	0.17	—
Insecta	0.95	54 783	0.56	380	0.32	47	0.26	27
Chondrichthyes	1.10	3961	0.59	119	0.39	14	0.33	8
Actinopterygii	0.85	122 390	0.61	—	0.59	—	0.56	1218
Amphibia	1.11	3405	0.86	387	0.62	89	0.54	48
Sauropsida	0.82	93 654	0.63	1082	0.50	205	0.44	102
Aves	0.87	59 457	0.63	1051	0.52	196	0.48	118
Mammalia	0.95	311 462	0.73	8531	0.53	674	0.49	313
Diet groups								
Carnivores	0.88	143 962	0.66	2583	0.58	507	0.55	280
Herbivores	0.97	274 108	0.64	2531	0.40	153	0.36	73
Omnivores	0.91	174 174	0.64	5589	0.63	1935	0.59	443
Other	0.99	25 743	0.68	304	0.56	72	0.52	43

where i and j denote trophic levels of species in a community ($i > j$); a_{ij} is the number of species interactions between trophic levels i and j; and m is the number of interactions within the community. Luna et al. (2020) considered Eq. 10 only for bipartite networks (two-trophic-level communities), but Eq. 10 can be extended to more complex communities and networks (Ulanowicz 2004, Shavit and Ellison 2021).

Equation 10 requires data from more than one trophic level, but current microbiome datasets usually have abundance data for only one trophic level (e.g. bacterial microbiome or virome). As a first effort to using Luna et al.'s (2020) approach to measuring heterogeneity of the AGMs, we built core-periphery networks (CPNs) of the AGM microbial communities in orders of animal hosts using the approach of Ma and Ellison (2019) and Li and Ma (2020). We then treated 'core' and 'periphery' as analogs to trophic levels and measured heterogeneity in two ways. First, we considered a two-level CPN with three possible interaction types — core–core, core–periphery or periphery–periphery — but without distinguishing interaction strengths (e.g. positive or negative correlations implying, respectively, positive or negative effects). Second, we used the same two-level CPN but added the sign of interaction strengths (positive or negative) to the interaction types (Fig. 2). Calculations were done after modifying Eq. 10 to use Hill numbers to measure the heterogeneity of the CPN:

$$ {}^{q}H_2 = \left(\sum_{i=1}^{m} \sum_{j=1}^{n} p_{ij}^{q} \right)^{1/(1-q)} \tag{11} $$

Table 5. Parameter estimates for the diversity–area relationship (DAR) for $q=0$ (species richness) fit using the linearized version power law with exponential cut-off model (Eq. 6). See the Supporting information for additional parameter estimates and model fits for the individual animal species used for these regional summaries.

	Diet group (*N)									
	Carnivore (19)		Herbivore (26)		Omnivore (30)		Other (3)		Class mean	
Class (*N)	z	D_{max}	z	D_{max}	z	D_{max}	z	D_{max}	z	D_{max}
Chromadorea (2)	—	—	—	—	—	—	0.855	2,341	0.855	2341
Arachnida (0)	—	—	—	—	—	—	—	—	—	—
Malacostraca (0)	—	—	—	—	—	—	—	—	—	—
Insecta (15)	—	—	0.752	7426	0.829	3281	1.018	5,651	0.866	5453
Chondrichthyes (1)	1.155	—	—	—	—	—	—	—	1.155	—
Actinopterygii (13)	0.894	12 117	0.467	1279	0.931	2757	—	—	0.764	5384
Amphibia (1)	0.937	1728	—	—	—	—	—	—	0.937	1728
Sauropsida (5)	0.764	10 741	0.774	17 063	0.885	14 121	—	—	0.808	13 974
Aves (9)	—	—	0.865	1582	0.874	7602	—	—	0.870	4592
Mammalia (32)	0.845	3176	1.004	503 004	0.855	4684	—	—	0.901	170 288
Diet group mean	0.919	6940	0.772	106 071	0.875	6489	0.937	3996		

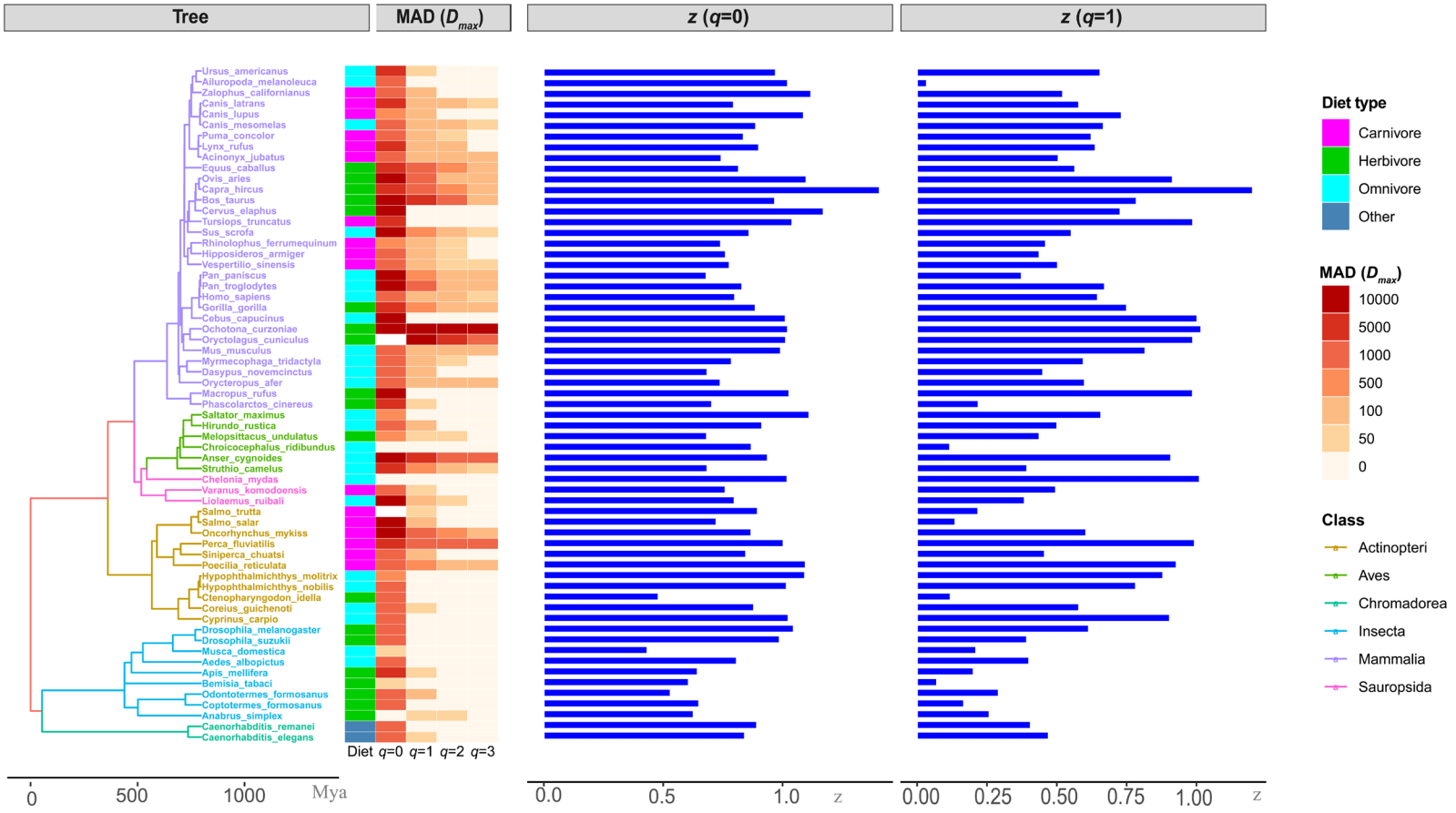

Figure 5. Correspondences between the estimated taxon age (phylogenetic timeline, PT) of 63 animal species (far left), maximum potential diversity ${}^{q}D_{\max}$ of their AGMs for $q \in \{0, 1, 2, 3\}$ (heat map; center left), and the diversity scaling parameter (z) for the AGMs at $q = 0$ (horizontal bar chart; center right) and $q = 1$ (horizontal bar chart; far right). See the Supporting information for parameter estimates, measures of fit, and p-values for the AGM diversity–area relationship (DAR) for each of these species.

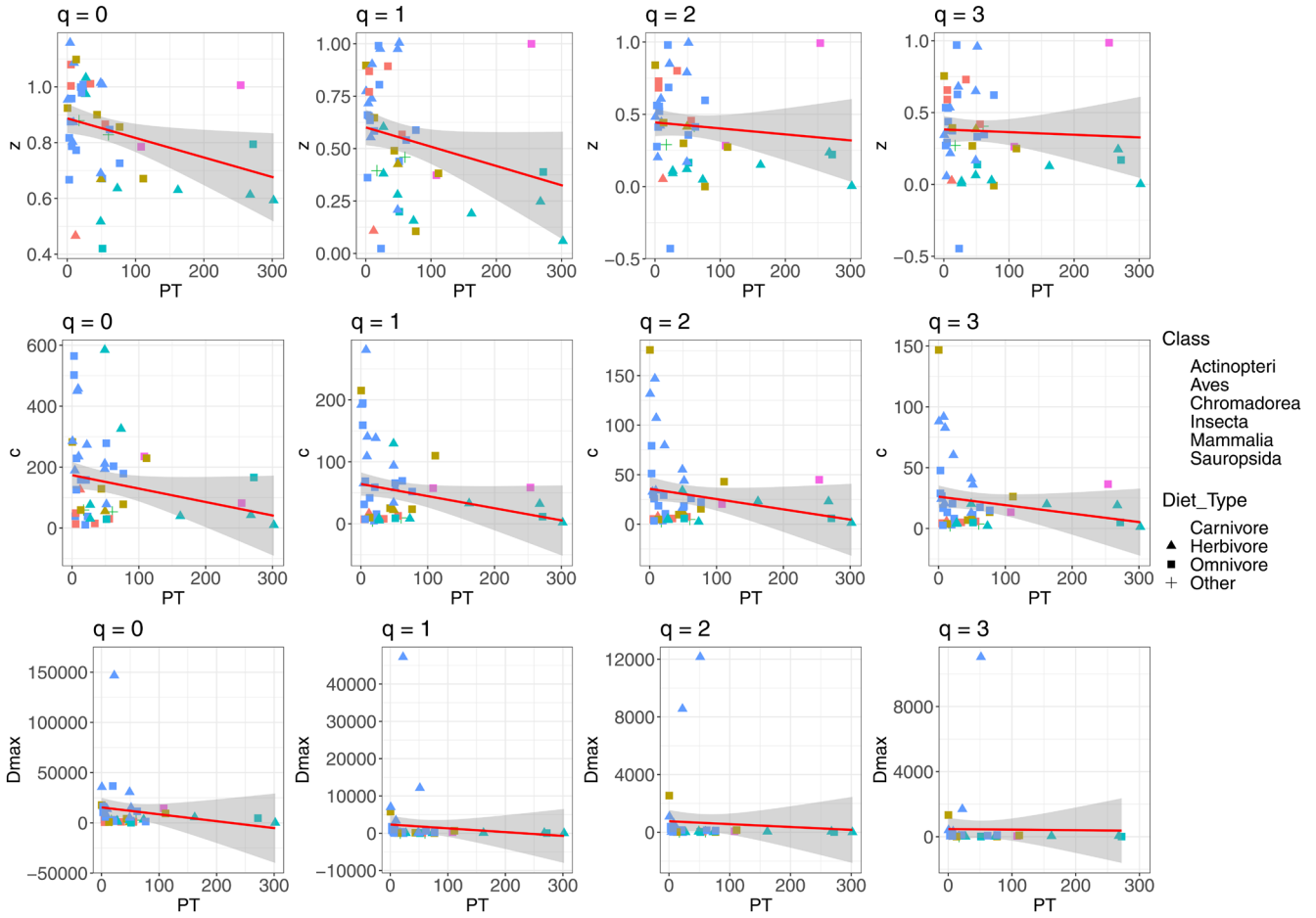

Figure 6. The relationships between estimated taxon age (phylogenetic timeline, PT) and the parameters and estimates from the diversity–area relationship (DAR) of the animal-gut microbiomes (AGMs) for $q \in \{0, 1, 2, 3\}$. The four columns of panels are for the four values of q. The top row of panels plots z versus PT; the second row plots c versus PT; and the third row plots the estimate of maximum global diversity D_{max} versus PT. Note that y-axis values change on plots within rows. See the Supporting information for the correlation coefficients and associated p-values.

where p_{ij} is the proportion of the interactions between type i and j, m is the strength of interaction types (here, m = 2, for positive or negative correlations), and n is the number of interaction types in our simplified CPN (here, n = 3, for intra-core, intra-periphery and inter-core-periphery links). Our intent here was to test whether heterogeneity measured using the extended TPL (Eq. 3) is correlated with heterogeneity measured as interaction diversity (Eq. 11), at least in a CPN.

Table 6. Parameters of the general diversity–time–area relationship (DTAR). Eq. 9 was fitted to the Hill-number diversity of the AGMs for orders $q \in \{0, 1, 2, 3\}$, animal taxon age (T in Eq. 9) and diet group as a proxy for area (A in Eq. 9).

q	w (time)	z (area)	ln(c)	R^2	p-value
0	1.26 (0.014)	0.32 (0.074)	6.08 (0.078)	0.90	< 0.001
1	1.46 (0.017)	0.46 (0.067)	2.38 (0.095)	0.92	< 0.001
2	1.32 (0.010)	0.30 (0.054)	0.97 (0.067)	0.92	< 0.001
3	1.20 (0.007)	0.26 (0.050)	0.65 (0.058)	0.90	< 0.001

Results

Heterogeneity of the AGM

Heterogeneity at the community scale

All estimates of the heterogeneity parameter b from the linearized version of Eq. 2 ($\ln(V_i) = b\ln(m_i) + \ln(a)$) were > 1, indicating that the AGM was heterogeneous and spatially non-random across all animal species and diet groups (Fig. 3). The scaling parameter b was significantly associated with estimated taxon age (phylogenetic timeline PT; Spearman's r = 0.20, p = 0.04; Fig. 3). In addition, b-value fits a power-law statistical distribution (K = 4.263; p = 0.759), suggesting a highly skewed distribution of the b-values.

Animal class was significantly associated with b ($H_{9,122}$ = 21.55, p = 0.01), but diet type ($H_{3,122}$ = 1.66, p = 0.65) and the class × diet type interaction ($H_{9,122}$ = 6.03, p = 0.74) were not (Table 1). The grand means of b and ln(a) were 2.233 and 5.968, respectively (Table 1).

Table 7. Species heterogeneity ${}^{q}H_2$ (Eq. 11) for $q \in \{0, 1, 2, 3\}$ and the parameter b from the extension of Taylor's power law (Eq. 3) in the core–periphery networks of the AGMs in taxonomic orders of animal hosts.

		Species heterogeneity ${}^{q}H_2$				
Class	Order	$q=0$	$q=1$	$q=2$	$q=3$	b
Nematoda	Rhabditida	2	1.505	1.322	1.256	1.969
Insecta	Blattodea	6	4.029	3.364	3.074	4.951
	Cingulata	5	2.777	2.609	2.511	0.981
	Coleoptera	3	2.018	1.679	1.547	1.682
	Diptera	3	2.385	2.005	1.814	1.864
	Hemiptera	5	2.886	2.205	1.952	1.568
	Hymenoptera	4	2.903	2.546	2.423	2.361
	Lepidoptera	4	3.572	3.240	3.000	2.012
	Orthoptera	3	2.425	2.243	2.173	1.681
Arachnida	Araneae	3	2.453	2.237	2.136	2.180
Malacostraca	Amphipoda	3	2.807	2.640	2.507	2.486
	Decapoda	3	2.239	1.838	1.664	1.865
Chondrichthyes	Carcharhiniformesmes	3	2.681	2.505	2.408	2.075
Actinopterygii	Acanthuriformes	3	2.198	2.018	1.941	2.497
	Centrarchiformes	5	2.614	2.375	2.247	2.059
	Cichliformes	6	3.036	2.668	2.499	2.092
	Cypriniformes	5	3.751	3.064	2.690	3.037
	Salmoniformes	3	2.173	1.810	1.655	1.601
Amphibia	Anura	3	2.512	2.234	2.078	1.280
Reptilia	Squamata	4	1.915	1.559	1.438	1.648
Aves	Anseriformes	3	2.792	2.615	2.476	1.438
	Charadriiformes	4	3.310	2.937	2.719	2.350
	Columbiformes	6	2.611	2.109	1.917	1.902
	Passeriformes	4	2.819	2.269	2.027	1.841
	Psittaciformes	2	1.854	1.742	1.664	1.489
	Struthioniformes	5	2.847	2.599	2.437	1.741
Mammalia	Carnivora	3	1.798	1.444	1.340	1.862
	Chiroptera	3	2.094	1.694	1.541	1.481
	Diprotodontia	6	4.476	4.054	3.845	2.509
	Perissodactyla	3	2.768	2.607	2.498	1.188
	Pilosa	4	2.459	2.146	1.980	2.336
	Primates	4	2.519	2.261	2.129	1.524
	Proboscidea	3	2.109	1.753	1.607	2.091
	Rodentia	3	1.777	1.451	1.351	1.903
	Tubulidentata	5	2.394	2.033	1.858	1.188

Global-scale heterogeneity

Considering the entire AGM across all species without regard to diet group or taxonomic class, $b = 1.645$ and $\ln(a) = 6.325$ ($p < 0.001$; Fig. 4A).

Heterogeneity at regional (landscape) scales

At the regional scales of taxonomic classes and diet groups (Fig. 1), heterogeneity was lower than community-scale heterogeneity (Table 2, Fig. 4B, 4C). Among taxonomic classes, b ranged from 1.089–2.009 (mean = 1.592), with invertebrates ($b = 1.448$) having, on average, lower values of b than vertebrates ($b = 1.713$) (Table 2, Fig. 4B). Among diet types, b ranged from 1.257–1.759 (mean = 1.551) and was ordered as herbivore > omnivore > carnivore > other (Table 3, Fig. 4C).

Diversity of the AGM

Diversity–area relationships of the AGM at the community scale

At the community scale and across all samples, $z = 0.91$ and estimated global species richness ${}^{0}D_{max} > 600\ 000$ OTUs (Table 4; first row). Within classes and diet groups, the scaling parameter (z) of the DAR (Eq. 5, 6) for species richness ($q = 0$) ranged from 0.76 (for carnivorous Sauropsida) to 1.16 (for carnivorous Chondrichthyes) and estimated potential AGM richness (D_{max} in Eq. 7) ranged from 1728 OTUs (in carnivorous Amphibia) to >500 000 OTUs (in herbivorous Mammalia) (Table 5). The estimated maximum Hill-number diversity ${}^{1}D_{mzx}$ was just over 8000 common or abundant species, and ${}^{2}D_{mzx}$ was ≈ 800 highly abundant or dominant species (Table 4; first row). For all diversity orders $q \in \{0, 1, 2, 3\}$, neither the DAR parameters nor the ratio of local (community scale) to global-scale (all AGMs) diversity (${}^{q}LGD$; Eq. 8) was significantly related to taxonomic class, diet type, or their interaction ($p > 0.1$, all cases).

Parallels between phylogenetic relationships of animal hosts, their AGMs, and the scaling parameters of their community-level DARs are illustrated in Fig. 5. All associations between estimated taxon age (PT) and the DAR parameters z, c and D_{max} were negative (Fig. 6), but these correlations were statistically significant ($p < 0.05$) only for z versus PT for $q = 0$ and $q = 1$; c versus PT for $q = 0$, and D_{max} versus PT for $q = 1$ and $q = 2$.

Diversity–area relationships of the AGM at the regional scale

At the regional scales of taxonomic class and diet type, the ordering of ${}^{q}D_{max}$ values (Table 4) and the scaling coefficients z (Table 5) of the AGM DARs paralleled those at the community scale. Estimated maximum species richness, ${}^{0}D_{max}$, of the AGMs of the animals with different diets were ≈ 274 000 for herbivores, 174 000 for omnivores, 144 000 for carnivores, and 25 000 for 'others' (Table 4).

The importance of taxon age for the DAR

The joint relationship between phylogeny and diversity of the AGM within diet types was fit well by the bivariate power-law (Eq. 9; $p < 0.001$). The scaling parameters (w for phylogeny and z for diet) was highest at diversity order $q = 1$ and the ratio of w/z ranged from 3.2 for $q = 1$ to 4.6 for $q = 3$ (Table 6).

Linking diversity and heterogeneity with interactions

Like ${}^{0}H$, heterogeneity of order $q=0$ (${}^{0}H_2$ from Eq. 11) measures the 'richness' of interactions which in this case is the number of linkage types in a CPN (out of six possible: core–core, core–periphery, periphery–periphery, each with either a positive or negative sign). Across 35 orders of host animals, ${}^{0}H_2$ ranged from 2 to 6 (Table 7). For $q > 0$, the range of ${}^{q}H_2$ was 1.2–4.5 (Table 7).

For all q, ${}^{q}H_2$ was significantly correlated with b (values in last column of Table 7), our measure of heterogeneity based on the extended TPL (Eq. 3). For $q = 0$, $r=0.47$ ($p=0.03$); for $q = 1$, $r=0.62$ ($p=0.001$); for $q = 2$, $r=0.54$ ($p=0.003$); and for $q = 3$, $r=0.58$ ($p=0.009$). However, b as a measure of heterogeneity was not significantly correlated with the diversity scaling parameter z for any order q ($r = -0.09$, -0.06, -0.04 and -0.03 for $q \in \{0, 1, 2, 3\}$, respectively; $p > 0.4$, all cases), illustrating that heterogeneity and diversity scaling reflect two independent aspects of AGM.

Discussion

Diversity and heterogeneity are both properties of groups of populations or species, but they have important differences (Shavit and Ellison 2021). Diversity reflects the number of discrete types whereas heterogeneity also includes interactions among the diverse objects. Information-theoretic ('entropy') measures such as Hill numbers suffice to measure diversity (Chao et al. 2014a, Chao and Colwell 2022), but corresponding measures of heterogeneity are still being developed (Luna et al. 2020, Shavit and Ellison 2021). Our analysis of diversity and heterogeneity of the animal-gut microbiome (AGM) suggests that diversity is shaped primarily by ecological processes, whereas heterogeneity is shaped primarily by evolutionary processes. This conclusion aligns with an extension of Taylor's (1981a, b, 1984, 1986) classic theories of population regulation (Taylor 1981a, b, Taylor 1984, 1986) in which spatial movement (an evolutionary characteristic) drives population aggregation (an ecological process; b in Eq. 1) in space and time.

Our extensions of Taylor's power law and Luna's measure of interaction diversity (heterogeneity) fit well the AGM datasets measured at three spatiotemporal scales of animal hosts. We estimated the total potential richness of the AGM, ${}^{0}D_{max}$, to be ≈ 600 000 OTUs, of which ≈ 10% were abundant or common (${}^{1}D_{max} \approx 8000$) and ≈ 1% were highly abundant or dominant (${}^{2}D_{max} \approx 800$). The maximum variation (values of w and z in Eq. 9) among taxonomic classes and diet types were highest common species (i.e. for diversity order $q=1$); w/z ranged from ≈ 3–4, suggesting that phylogeny is more important than diet type for AGM diversity. Similarly, our data suggest that phylogeny has a stronger effect on heterogeneity than does diet type.

However, these conclusions should be interpreted cautiously. Most importantly, the parameters we estimated — b, z, c and D_{max} — are not direct measures of heterogeneity or diversity. Rather, b and z are scaling parameters; b measures the rate of change of variance with respect to the mean (on a log-scale), whereas z measures the change of diversity across area (space) and serves as a proxy for beta diversity. c and D_{max} are, respectively, estimators of average local (alpha) diversity and potential ('dark') diversity. Secondarily, diet types also are evolved traits, and the associations between the AGM and phylogenetic relationships, taxon age, and diet type are likely to be more complex than can be captured directly in coarse taxonomic classifications or ANOVA tables.

Nonetheless, our data suggest that taxon age is a power lens through which to discern scaling patterns in microbial diversity and heterogeneity. We hypothesize that the identity of individual host taxa, as representatives of singular evolutionary events, has little effect on scaling of microbial diversity. In contrast, taxon age better reflects evolutionary relationships emerging across taxa over time. In support of this hypothesis, we observed that z (a proxy for beta-diversity) of the AGM is negatively correlated with the estimated taxonomic age of the host-animal species. This negative correlation implies that younger species generally host more diverse AGM communities. In contrast, b (a proxy for the scaling relationship of heterogeneity) of the AGM is positively correlated with estimated taxon age of the host-animal species, implying that the AGMs of younger species have lower heterogeneity scaling, potentially more stable.

We propose that the differences between diversity and heterogeneity reflect processes occurring at different time scales. From their studies on insect population dynamics, Taylor (1981a, b) and Taylor (1986) suggested that b is a species-specific characteristic reflecting spatial behavior that is shaped by long-term evolutionary processes. Metagenomics has allowed these population-level analyses to be extended to communities and meta-communities (Ma 2012, 2015, Ma and Taylor 2020) and reinforces the conclusion that heterogeneity (often referred to as aggregation in population ecology) primarily reflects evolved behavioral traits and interactions, whereas diversity reflects the spatiotemporal redistribution or fluctuation of species abundances in ecological time. In short, we hypothesize that heterogeneity reflects long-term

evolutionary processes whereas diversity reflects shorter-term ecological dynamics.

Finally, our results that z and b are uncorrelated at all diversity orders $q \in \{0,1,2,3\}$ support the conclusions of Shavit and Ellison (2021) that diversity and heterogeneity are two different properties of communities at any scale. Although bivariate power-law distributions, which we used for modeling both heterogeneity and diversity, share the properties of log-linear scaling, self-similarity or scale invariance, and 'no-averages' (Stumpf and Porter 2012), successfully using the same type of equations to model two datasets does imply that they share similar scaling mechanisms.

Acknowledgements – We thank Robin Taylor for helpful and constructive comments on the initial submission of the manuscript. *Funding* – This study received funding from the National Science Foundation of China (grant numbers 31970116 and 72274192). AME's initial work on this project was supported by a Global Fellowship Award from the University of St Andrews. Additional support during manuscript preparation was provided by a Charles Bullard Fellowship in Forest Research to ZSM.

Author contributions

Zhanshan (Sam) Ma: Conceptualization (equal); Data curation (equal); Formal analysis (equal); Investigation (equal); Methodology (equal); Writing – original draft (equal); Writing – review and editing (equal). **Aaron M. Ellison:** Conceptualization (equal); Methodology (equal); Writing – review and editing (equal).

Data availability statement

All datasets analyzed in the study are available in public domain; the sequence accession numbers and published sources are listed in Ma and Ellison 2024 and were analyzed in different ways by Ma (2021) and Ma et al. (2022), Ma and Li 2024, Ma and Shi (2024). Reanalysis of these data does not require approval by Institutional Review Boards (IRBs) or Institutional Animal Use and Care Committees (IACUCs). Code used to analyze these data are also available in previously published work (Ma 2018a, Li and Ma 2019). For detailed information, please visit: https://harvardforest1.fas.harvard.edu/exist/apps/datasets/showData.html?id=HF448.

Supporting information

The Supporting information associated with this article is available with the online version.

References

Allesina, S. and Tang, S. 2015. The stability-complexity relationship at age 40: a random matrix perspective. – Popul. Ecol. 57: 63–75.

Bolyen, E. et al. 2019. Reproducible, interactive, scalable and extensible microbiome data science using QIIME 2. – Nat. Biotechnol. 37: 852–857.

Chao, A. and Colwell, R. K. 2022. Biodiversity: concepts, dimensions, and measures. – In: Loreau, M., Hector, A. and Isbell, F. (eds), The ecological and societal consequences of biodiversity loss. ISTE Ltd. and John Wiley & Sons, Inc., pp. 25–46.

Chao, A., Chiu, C. H. and Jost, L. 2014a. Unifying species diversity, phylogenetic diversity, functional diversity and related similarity and differentiation measures through Hill numbers. – Annu. Rev. Ecol. Evol. Syst. 45: 297–324.

Chao, A., Gotelli,N. G., Hsieh, T. C., Sander, E. L., Ma, K. H., Colwell, R. C. and Ellison, A. M. 2014b. Rarefaction and extrapolation with Hill numbers: a framework for sampling and estimation in species biodiversity studies. – Ecol. Monogr. 84: 45–67.

Cohen, J. E. and Saitoh, T. 2016. Population dynamics, synchrony, and environmental quality of Hokkaido voles lead to temporal and spatial Taylor's laws. – Ecology 97: 3402–3413.

Connor, E. F. and McCoy, E. D. 1979. The statistics and biology of the species–area relationship. – Am. Nat. 113: 791–833.

Ellison, A. M. 2010. Partitioning diversity. – Ecology 91: 1962–1963.

Hammill, E., Hawkins, C. P., Greig, H. S., Kratina, P., Shurin, J. B. and Atwood, T. B. 2018. Landscape heterogeneity strengthens the relationship between beta-diversity and ecosystem function. – Ecology 99: 2467–2475.

Huffaker, C. B. 1958. Experimental studies on predation: dispersal factors and predator–prey oscillations. – Hilgardia 27: 343–383.

Kolasa, J. and Pickett, S. T. A. (eds) 1991. Ecological heterogeneity. – Springer.

Kumar, S., Stecher, G., Suleski, M. and Hedges, S. B. 2017. TimeTree: a resource for timelines, timetrees and divergence times. – Mol. Biol. Evol. 34: 1812–1819.

Levin, S. A. 1992. The problem of pattern and scale in ecology. – Ecology 73: 1943–1967.

Li, H. and Reynolds, J. F. 1995. On definition and quantification of heterogeneity. – Oikos 73: 280–284.

Li, L. W. and Ma, Z. S. 2019. Comparative power law analysis for the spatial heterogeneity scaling of the hot-spring and human microbiomes. – Mol. Ecol. 28: 2932–2943.

Li, W. D. and Ma, Z. S. 2020. Dominance network analysis of the healthy human vaginal microbiome not dominated by *Lactobacillus* species. – Comp. Struct. Biotechnol. J. 18: 3447–3456.

Luna, P., Corro, E. J., Antoniazzi, R. and Dáttilo, W. 2020. Measuring and linking the missing part of biodiversity and ecosystem function: the diversity of biotic interactions. – Diversity 12: 86.

Ma, Z. S. 2012. A note on extending Taylor's Power Law for characterizing human microbial communities: inspiration from comparative studies on the distribution patterns of insects and galaxies, and as a case study for medical ecology. – arXiv (preprint).

Ma, Z. S. 1991. Further interpreted Taylor's Power Law and population aggregation critical density. – Trans. Ecol. Soc. China 1: 284–288.

Ma, Z. S. 2015. Power law analysis of the human microbiome. – Mol. Ecol. 24: 5428–5445.

Ma, Z. S. 2018a. DAR (diversity–area relationship): extending classic SAR (species–area relationship) for biodiversity and biogeography analyses. – Ecol. Evol. 8: 10023–10038.

Ma, Z. S. 2018b. Diversity time-period and diversity–time–area relationships exemplified by the human microbiome. – Sci. Rep. 8: 7214.

Ma, Z. S. 2021. Cross-scale analyses of animal and human gut microbiome assemblies from metacommunity to global landscape. – mSystems 6: e0063321.
Ma, Z. S. and Ellison, A. M. 2018. A unified concept of dominance applicable at both community and species scales. – Ecosphere 9: e02477.
Ma, Z. S. and Ellison, A. M. 2019. Dominance network analysis provides a new framework for studying the diversity–stability relationship. – Ecol. Monogr. 89: e01358.
Ma, Z. S. and Taylor, R. A. J. 2020. Human reproductive system microbiomes exhibited significantly different heterogeneity scaling with gut microbiome, but the intra-system scaling is invariant. – Oikos 129: 903–911.
Ma, Z. S. and Ellison, A. M. 2021. Toward a unified diversity–area relationship (DAR) of species and gene diversity illustrated with the human gut metagenome. – Ecosphere 12: e03807.
Ma, Z. and Ellison, A. 2024. Animal gut microbiome (AGM) Data from 91 published studies for 224 animal species. – Harvard Forest Data Archive: HF448 (v.1). Environmental Data Initiative: https://doi.org/10.6073/pasta/b4e1b51f686adaee7f637d1b0049be5c
Ma, Z. S. and Li, L. W. 2024. Biodiversity metrics on ecological networks: demonstrated with animal gastrointestinal microbiomes. – Zool. Res. Divers. Conserv. 1: 51–65.
Ma, Z. S. and Shi, P. 2024. Critical complex network structures in animal gastrointestinal tract microbiomes. – Anim. Microbiome 6: 23.
Ma, Z. S., Li, W. D. and Shi, P. 2022. Microbiome–host-phylogeny relationships in animal gastrointestinal tract microbiomes. – FEMS Microbiol. Ecol. 98: fiac021.
Magurran, A. E. and McGill, B. J. 2011. Biological diversity: frontiers in measurement and assessment. – Oxford Univ. Press.
Mangiafico, S. S. 2024. rcompanion: functions to support extension education program evaluation, ver. 2.4.35. – https:CRAN.R-project.org/package=rcompanion/.
May, R. M. 1973. Stability and complexity in model ecosystems. – Princeton Univ. Press.
McCann, K. S. 2000. The diversity–stability debate. – Nature 405: 228–233.
Oh, J., Byrd, A., Park, M., Kong, H. and Segre, J. 2016. Temporal stability of the human skin microbiome. – Cell 165: 854–866.
Paradis, E., Claude, J. and Strimmer, K. 2004. APE: analyses of phylogenetics and evolution in R language. – Bioinformatics 20: 289–290.
Partel, M. R., Szava-Kovats, R. and. Zobel, M. 2011. Dark diversity: shedding light on absent species. – Trends Ecol. Evol. 26: 124–128.
Real, R., Barbosa, A. M. and Bull, J. W. 2017. Species distributions, quantum theory, and the enhancement of biodiversity measures. – Syst. Biol. 66: 453–462.
Rosenzweig, M. L. 1995. Species diversity in space and time. – Cambridge Univ. Press.
Shavit, A. and Ellison, A. M. 2021. Diversity is conflated with heterogeneous collectives. – J. Philos. 118: 525–548.
Stumpf, M. P. H. and Porter, M. A. 2012. Critical truths about power laws. – Science 335: 665–666.
Taylor, L. R. 1961. Aggregation, variance and the mean. – Nature 189: 732–735.
Taylor, L. R. 1984. Assessing and interpreting the spatial distributions of insect populations. – Annu. Rev. Entomol. 29: 321–357.
Taylor, L. R. and Taylor, R. A. J. 1977. Aggregation, migration and population mechanics. – Nature 265: 415–421.
Taylor, L. R. 1986. Synoptic dynamics, migration and the Rothamsted insect survey. – J. Anim. Ecol. 55: 1–38.
Taylor, R. A. J. 1981a. The behavioural basis of redistribution: 1. The DELTA-model concept. – J. Anim. Ecol. 50: 573–586.
Taylor, R. A. J. 1981b. The behavioural basis of redistribution: 2. Simulations of the DELTA-model. – J. Anim. Ecol. 50: 587–604.
Taylor, R. A. J. 2019. Taylor's power law: order and pattern in nature. – Academic Press.
Turner, M. G. and Gardner, R. H. 2015. Landscape ecology in theory and practice: pattern and process. – Springer.
Ulanowicz, R. E. 2004. Quantitative methods for ecological network analysis. – Comp. Biol. Chem. 28: 321–339.
Yu, G., Smith, D. K., Zhu, H., Guan, Y. and Lam, T. T.-Y. 2017. ggtree: an R package for visualization and annotation of phylogenetic trees with their covariates and other associated data. – Methods Ecol. Evol. 8: 28–36.